Uncertainty in Future Projections of Precipitation Decline over Mesopotamia

YEON-WOO CHOI[a] AND ELFATIH A. B. ELTAHIR[a]

[a] *Ralph M. Parsons Laboratory, Massachusetts Institute of Technology, Cambridge, Massachusetts*

ABSTRACT: For millennia, Mesopotamia was blessed by enough water supplied by the Tigris and Euphrates Rivers. However, the dwindling freshwater resource is no longer enough. In the future, climate change coupled with a growing population could considerably exacerbate the current water deficit. Based on simulations by carefully selected global and regional climate models, we conclude that these river basins may possibly face further water shortages (mainly due to a reduction in spring-season precipitation) in the next few decades (2021–50) under a scenario of high emissions of greenhouse gases. However, there is no consensus among models regarding these near-term (2021–50) projections of change in precipitation, and society is likely to face the challenge of how to prepare for this uncertain future. The story is different for the late decades of this century: we project, with significantly more confidence, a robust decrease in wet-season (winter to spring) precipitation over the headwaters of these river basins, worsening future water deficits and implying a century-long drying trend over Mesopotamia. Possible physical mechanisms are proposed and discussed. As global warming progresses, higher sea level pressure, centered on the Mediterranean Sea, will likely make upstream storms less frequent and weaker, leading to drying over Mesopotamia. Further, projections show a poleward migration of the fewer Mediterranean storm tracks, decreasing the frequency of storms that penetrate into Mesopotamia. Implementing a global net-zero carbon emissions policy by midcentury could mitigate the severity of the projected droughts in this region.

KEYWORDS: Precipitation; Storm tracks; Climate change; Climate models

1. Introduction

The Tigris and Euphrates Rivers, originating from mountainous regions of eastern Turkey, historically played an important role in sustaining the modern civilizations in Mesopotamia, known as the cradle of civilization (Fig. 1; see also Fig. S1 in the online supplemental material). The two rivers have helped people to secure sufficient freshwater for irrigation and domestic uses for a long time. However, droughts, ever-growing population, and anthropogenic activities (including upstream dam construction, expansion of irrigation, and groundwater pumping) led to severe water shortages that impact downstream communities (Voss et al. 2013; United Nations 2019; Yilmaz et al. 2019; Wu et al. 2020). In particular, a prolonged drought contributed to the unstable conditions in the region, causing tremendous economic costs and significant loss of human lives (Trigo et al. 2010; Kelley et al. 2015; Hochman et al. 2022). Without effective population control policy and transboundary cooperation on water management, the situation is expected to worsen in the coming years.

Climate change may have further exacerbated existing water scarcity in the eastern Mediterranean, with the most significant decline in the winter (Kelley et al. 2012, 2015; Wu et al. 2020;

Hochman et al. 2022; Fig. 2). One may argue that this drying from the late 1970s appears to be related to the positive phase of the North Atlantic Oscillation (NAO), the natural mode of climate variability (Cullen and deMenocal 2000; Fig. S2). However, some previous studies suggested that this decline in freshwater resources is more likely to be driven by anthropogenic climate change than natural variability (Kelley et al. 2012, 2015).

An increasing body of literature suggests, using models from phases 3 and 5 of the Coupled Model Intercomparison Project (CMIP3 and CMIP5), that the region is likely to experience increased aridity by 2100 (Giorgi 2006; Kitoh et al. 2008; Diffenbaugh and Giorgi 2012; Wu et al. 2020). Furthermore, regional modeling studies, providing additional details, also demonstrate the critical water scarcity situation projected for the same period of the late twenty-first century (Bozkurt and Sen 2013; Önol et al. 2014). A key question here is whether this trend will be detectable in the near-term future when the external anthropogenic forcing is relatively small. Less attention has been paid to near-term future changes in precipitation, which presents significant challenges for policymakers seeking to develop sound adaptation strategies for the near future.

Furthermore, a relevant question is how climate change may lead to dry signals in the Mesopotamian basins. According to previous studies, dry conditions around this region can be shaped by 1) an enhanced anticyclonic circulation over the Mediterranean related to climate change (Tuel and Eltahir 2020, 2021) and 2) a weaker midlatitude storm activity crossing the region (Evans 2009; Zappa et al. 2015a; Matsumura et al. 2019; Reale et al. 2021; Tuel et al. 2022). More specifically, Tuel and Eltahir (2020, 2021) proposed that a lengthening of the stationary wavelengths and contrasting warming
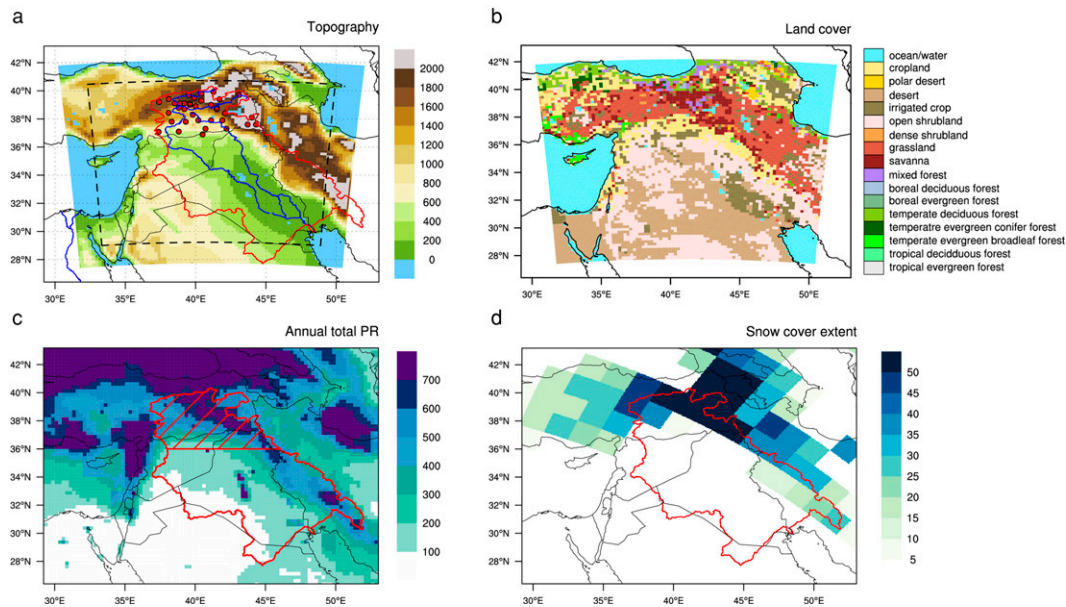

FIG. 1. (a) MRCM domain and topography (unit: m). The Mesopotamian basin is represented by the red line in (a). Red dots and blue lines in (a) denote the location of 36 weather stations and major rivers in the Mesopotamian basin, respectively. (b) Land-use distribution used for regional climate model simulations. Spatial distribution of (c) annual total rainfall (PR; unit: mm) and (d) satellite-based wet-season (November–May) snow-cover extent (unit: %). Superimposed hatching in (c) indicates the Mesopotamian headwaters.

between the Mediterranean Sea and surrounding land are important drivers of the enhanced anticyclonic anomaly, leading to the Mediterranean precipitation decline. They also suggested that the enhanced anticyclonic circulation may drive less frequent and/or weaker storms over the Mediterranean. Furthermore, several recent studies shed light on the causes of changes in midlatitude storm activity (which shape midlatitude precipitation regimes), such as an expanded tropical band (Seidel et al. 2008), a poleward shift of storm tracks (Yin 2005; Seidel et al. 2008; Peleg et al. 2015; Matsumura et al. 2019), and midlatitude warming (Lee et al. 2019; Matsumura et al. 2019) in the Atlantic Ocean. However, it is still unclear how future climate change will affect precipitation in Mesopotamia at the regional scale.

This study aims to fill these knowledge gaps based on analyses of carefully selected global and regional climate model simulations. We test the hypothesis that significant reductions in precipitation and associated water shortages may occur in Mesopotamia during the twenty-first century. We propose and test mechanisms that emphasize the impact of circulations changes, driving less frequent and weaker Mediterranean storms that propagate into Mesopotamia.

2. Data and methods

a. Global climate model simulations

State-of-the-art climate models are used in this study to project changes in water availability in Mesopotamia (see Table S1 in the online supplemental material). Based on the recommendations from McSweeney et al. (2015), this study adopts 18 CMIP5 models from the Intergovernmental Panel on Climate Change (IPCC) Fifth Assessment Report (AR5), with the best performance in reproducing key climate features (circulations, storm tracks, and annual cycles of temperature and precipitation) over the Mediterranean region. Also, we use all available CMIP6 models that provide 6-hourly data [temperature, winds, specific humidity, surface pressure, and sea surface temperature (SST)] for the period 1976–2100. In general, for each model, one ensemble member is used (see Table S1 in the online supplemental material). However, for some of the wind analysis, 35 ensemble members for MPI-ESM1-2-LR, HadGEM3-GC31-LL, and NorESM2-LM are used to eliminate internal variability, as described below. The CMIP5 projections are forced by representative concentration pathway (RCP) scenarios, and the CMIP6 simulations are based on shared socioeconomic pathway (SSP) scenarios. High (RCP8.5 and SSP5-8.5) and low emission scenarios (RCP2.6 and SSP1-2.6) are considered. Near-term (2021–50) and far-future (2071–2100) climate changes are analyzed compared to reference scenarios (1985–2014). All model output is regridded to a common $1° \times 1°$ grid.

b. Regional climate model and experimental design

We use the MIT Regional Climate Model (MRCM; Pal and Eltahir 2016), of which the dynamical core originated from the Abdus Salam International Centre for Theoretical Physics (ICTP) Regional Climate Model version 3 (RegCM3; Pal et al. 2007). Unlike RegCM3, the MRCM is coupled with Integrated Biosphere Simulator (IBIS; Foley et al. 1996), showing a better representation of land surface processes (Winter et al. 2009).
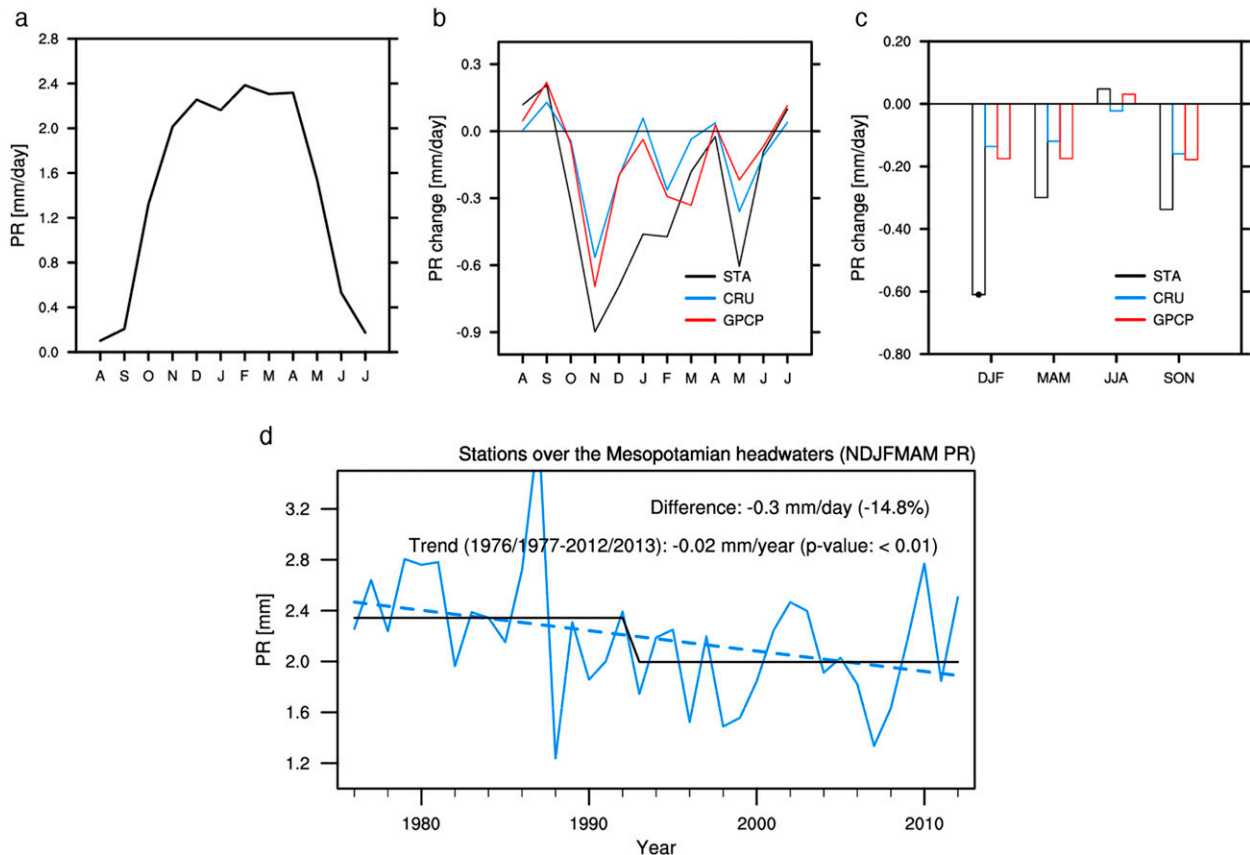
FIG. 2. (a) Seasonal cycle of precipitation (PR; unit: mm day^{-1}) over the Mesopotamian headwaters (CRU 1976–2014 average). (b) Observed changes in the PR seasonal cycle over the region derived from station observations (1995–2013 minus 1976–94), CRU (1995–2014 minus 1976–95), and GPCP (1997–2014 minus 1979–96). (c) As in (b), but for seasonal-mean values. The black dot in (c) indicates the season when the difference is statistically significant at the 5% level as determined by a two-sided Student's t test. (d) Time series of seasonally [November–May (NDJFMAM)] averaged PR (unit: mm) over the region for the period 1976/77–2012/13 derived from station observations. The best-fit linear regression line is shown in dashed blue in (d). Difference between first and last 20 years is represented by black horizontal lines in (d). The p value for the linear trend in (d) is based on the nonparametric Mann–Kendall test. Average precipitation across 36 weather stations (with equal weight given to each station; see Fig. 1a for the locations of stations) is used in (b)–(d).

Additionally, updated or newly developed physical schemes are incorporated into the MRCM (Marcella 2012; Marcella and Eltahir 2012; Gianotti 2012; Gianotti and Eltahir 2014a,b). Previous studies demonstrated that the MRCM could be applied for regional climate studies across various domains, including the Mediterranean region (Tuel and Eltahir 2020), North America (Winter et al. 2009), West Africa (Im et al. 2014a), Southwest Asia (Pal and Eltahir 2016; Choi and Eltahir 2022), South Asia (Im et al. 2017a; Choi et al. 2021), and the Maritime Continent (Im and Eltahir 2018).

To provide reliable regional climate change projections, it is necessary to rigorously evaluate the performance of global circulation models (GCMs; used to specify the boundary conditions for the MRCM) (Im et al. 2017a; Kang and Eltahir 2018). In this study, CMIP6 GCMs are carefully selected by considering their ability to capture the long-term average climate and its trends. As a result of the model evaluation,

13 models out of 30 CMIP6 models are able to reproduce the observed decrease in precipitation over the Mesopotamian headwaters (Fig. 3a). Among the 13 models, five models, including CMCC-CM2-SR5, ACCESS-CM2, IPSL-CM6A-LR, UKESM1-0-LL, and HadGEM3-GC31-MM, are excluded from further analysis because the ensemble member selected for each model (for dynamical downscaling) shows different behavior of precipitation trend compared to its multimember ensemble mean. Three models (CMCC-ESM2, BCC-CSM2-MR, and KACE-1-0-G) are further excluded due to the limited data availability. Also, NESM3, which fails to capture the seasonal cycle in precipitation, is excluded.

We finally selected three models that perform best: MPI-ESM1-2-LR (MPI), HadGEM3-GC31-LL (HAD), and NorESM2-LM (NOR) (Fig. S3). These three models have the least averaged root-mean-square error (RMSE) for temperature
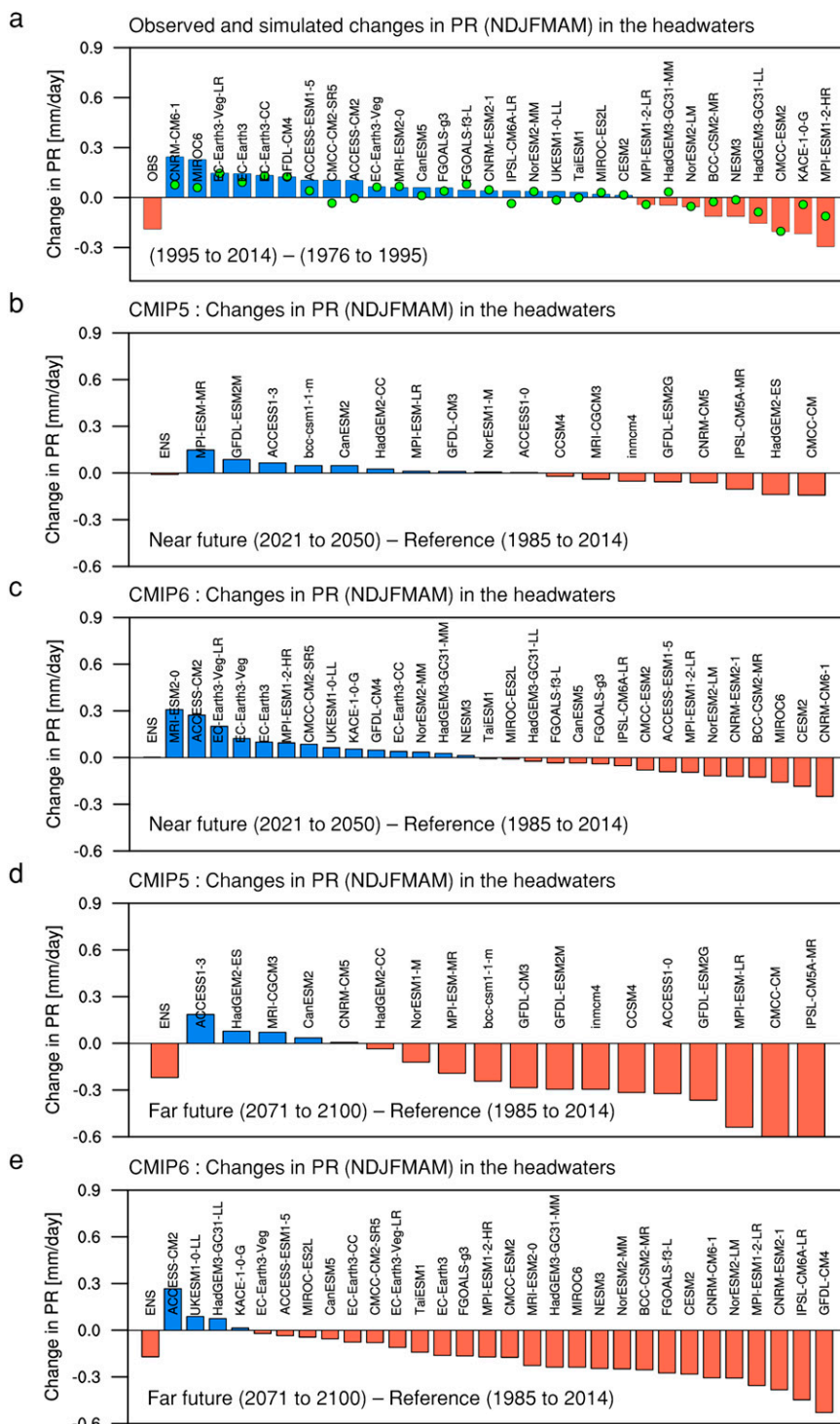
FIG. 3. (a) Observed and simulated changes (1995–2014 minus 1976–95) in seasonal [November–May (NDJFMAM)] mean precipitation (PR; unit: mm day^{-1}) over the Mesopotamian headwaters derived from CRU (OBS) and CMIP6 simulations. Projected near-term changes (2021–50 minus 1985–2014) in seasonal-mean PR over the region derived from (b) CMIP5 and (c) CMIP6 GCMs. (d),(e) As in (b) and (c), but for far future (2071–2100). The multimodel ensemble mean (ENS) is indicated in the left corner of (b)–(e). The selected one ensemble member per model is shown as a colored box in (a)–(e). Single-model multimember ensemble means (with equal weight given to each ensemble member) are indicated by green dots in (a).
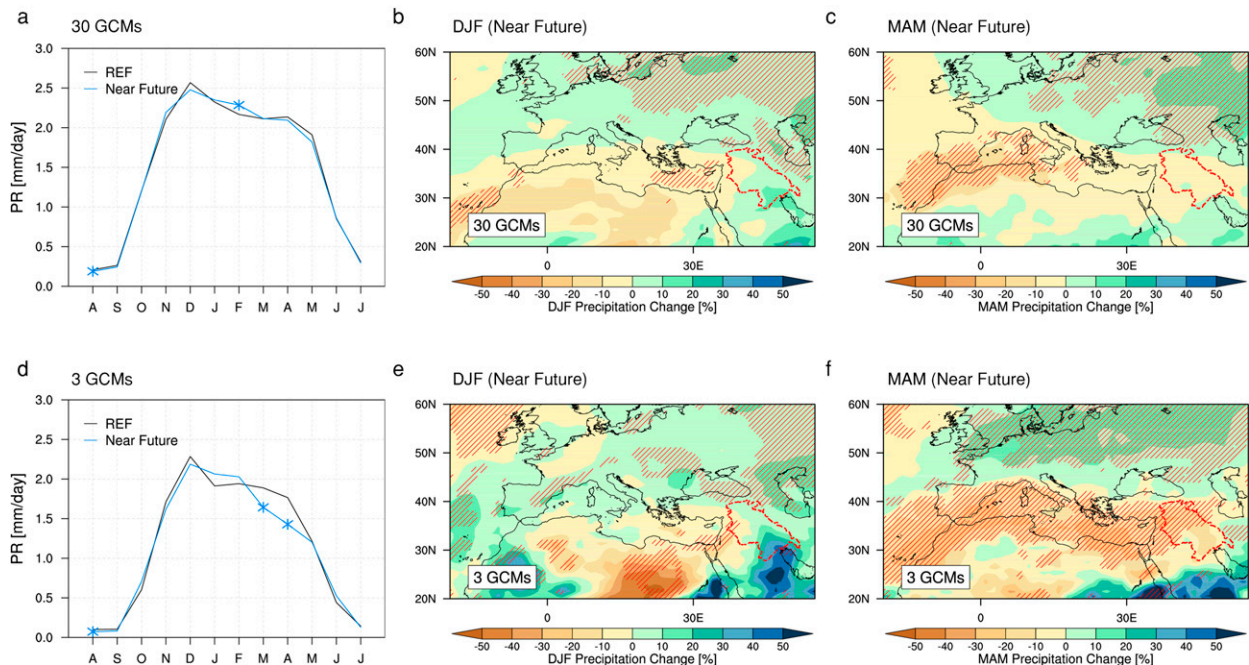
FIG. 4. The seasonal cycle of precipitation (PR; unit: mm day^{-1}) over the Mesopotamian headwaters for the reference (1985–2014) and near-future (2021–50) periods derived from the ensemble means of (a) 30 and (d) 3 CMIP6 GCMs. Projected changes in PR during (b) the winter (December–February) and (c) spring (March–May) derived from ensemble of 30 CMIP6 GCMs. (e),(f) As in (b) and (c), but for an ensemble of 3 CMIP6 GCMs. Asterisks in (a) and (d) indicate a month when the difference is statistically significant at the 5% level as determined by a two-sided Student's t test. Superimposed hatching in (b) and (c) indicates that more than 80% of models agree on the sign of the change. Superimposed hatching in (e) and (f) denotes agreement (100%) by three GCMs on the sign of the change.

and precipitation simulations (1985–2014) over the Mesopotamian headwaters. Note that only one model having the smallest RMSE is selected from each institution. Perhaps not surprisingly, the MRCM performs better than the driving GCMs in reproducing overall spatial variability of temperature and precipitation (Fig. S4). In particular, the MRCM can provide added value over the Mesopotamian headwaters by better representing the spatial distribution of precipitation (Fig. S4c).

The simulation domain is centered at 35°N, 41°E, covering the eastern Mediterranean region with a Lambert conformal projection (Fig. 1). The spatial resolution of the model is 20 km in both longitudinal and latitudinal directions. Climate simulations are conducted for the 1975–2050 period. Reference (1985–2014) and near-term future (2021–50) periods are mainly analyzed. The first year of each simulation is regarded as a spinup period and thus excluded from the analysis. Massive irrigation systems are well developed in Mesopotamia. Accordingly, implementing an irrigation module can improve the simulation of climate over the region (Marcella and Eltahir 2012). Water is only supplied in the first week of October–April to avoid excessive or unrealistic irrigated water (Im et al. 2014b; Im and Eltahir 2014).

The extratropical storms (i.e., synoptic-scale cyclones) are a critical atmospheric process, bringing a large amount of rainfall into the eastern Mesopotamia region (Marcella and Eltahir 2008). To understand the underlying mechanisms of projected change in precipitation, storm track activity is estimated using

daily kinetic energy, which is bandpass filtered to isolate events between 2 and 8 days, in line with Yin (2005). Also, individual storm events are detected as minima in sea level pressure (SLP) using a mesoscale eddy tracking algorithm (available at https://github.com/ecjoliver/stormTracking). This storm tracking algorithm is a modified form of the mesoscale ocean eddy tracking algorithm (Chelton et al. 2011).

To quantify the role of the zonal wind changes on the precipitation response to increasing atmospheric CO_2 concentration, a circulation index is defined as the difference between Europe (35°–50°N, 0°–50°E) and North Africa (20°–35°N, 0°–50°E) zonal winds at 700 hPa. This circulation index is closely related to an anomalous high pressure in the lower troposphere induced by climate change (see section 3d for details) and can be a proxy for lower-tropospheric geopotential height.

c. Observation data

Various precipitation datasets are obtained from the Climate Research Unit product (CRU; Harris et al. 2020), the Global Precipitation Climatology Project (GPCP; Adler et al. 2003), the Tropical Rainfall Measuring Mission (TRMM; Huffman et al. 2007), and the Global Historical Climatology Network (GHCN; Peterson and Vose 1997) at 36 weather stations around eastern Turkey (Fig. 1a). Satellite-based snow-cover extent is provided from the National Oceanic and Atmospheric Administration (NOAA) Climate Data Record (CDR) (Robinson et al. 2012). The NAO index is from the National
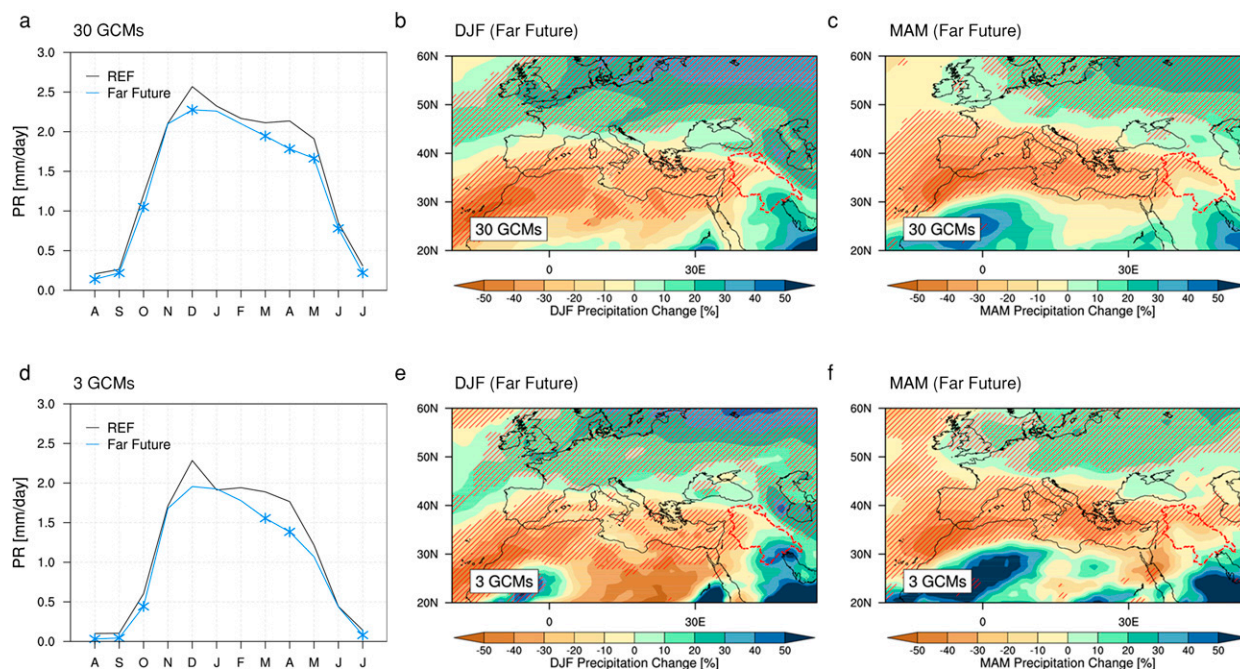
FIG. 5. As in Fig. 4, but for the far-future period (2071–2100).

Oceanic and Atmospheric Administration (NOAA) Climate Prediction Center (CPC; available at http://www.cpc.ncep.noaa. gov/). The 6-hourly storm track data are available at https:// github.com/ecjoliver/stormTracking.

3. Results

a. Observed changes in precipitation

Modern climate records from ground and satellite observations indicate the prolonged reduction in precipitation in Mesopotamia (Fig. 2). Northern Mesopotamia (characterized by the Mediterranean climate) receives the majority of annual precipitation (in the form of snow and rain) during the cold season (November–May; Figs. 1c,d and 2a), which largely determines the annual flow rate of the Tigris and Euphrates Rivers. Accumulated snow during winter begins to melt in spring, flowing into the downstream region and providing freshwater. In recent decades, wet-season precipitation has decreased by about 15% compared to the late 1970s, showing a continuing downward trend (p value < 0.01). The most significant decrease in precipitation is observed in winter, potentially related to anthropogenic climate change (Kelley et al. 2012).

b. Global climate projections

Precipitation response to near-term climate change remains uncertain based on climate projections from CMIP5 and CMIP6 models (Fig. 3). However, water deficit is projected to worsen in the Mesopotamian basin by the end of this century with high confidence, assuming business-as-usual greenhouse gas emissions scenarios (i.e., the RCP8.5 and SSP5-8.5 scenarios) (Fig. 3; see also Figs. S5 and S6). For the near-term future, nearly half of CMIP6 models (14 GCMs) project an overall increase in wet-

season precipitation, while the other half (16 GCMs) indicates a drying tendency. The CMIP5 models support a similar conclusion. For the far future, enhanced global warming will lead to a significant drying tendency in the sources of the rivers with a strong agreement between models (13 out of 18 CMIP5 models and 26 out of 30 CMIP6 models agree on the sign of the change). That is, the multimodel mean precipitation during the wet season is projected to decrease by about 0.2 mm day^{-1} by 2100 (RCP8.5: 13% with p value less than 0.01; SSP5-8.5: 8% with p value less than 0.01).

Based on the GCM projections, the spatial distribution of precipitation change presents four interesting features (Figs. 4 and 5): 1) there is a meridional dipole pattern of precipitation change, especially north of about 25°N; 2) this signal is more pronounced in the three selected models (which are assumed to provide more credible climate projections) than in all models, and in spring than in winter (particularly during the near-term future); 3) the precipitation response is proportional to the global warming levels (i.e., the signal-to-noise ratio becomes larger by the end of the twenty-first century as the climate change signal clearly emerges) (Figs. S5 and S6); and 4) the regions where most models (more than 80% of models) agree on the sign of the precipitation change become more widespread toward the end of the twenty-first century. At the regional scale, the three selected GCMs project a likely decrease in spring-season precipitation in a broad area extending from the Mediterranean to the headwaters of the Tigris and Euphrates Rivers in the coming decades. This tendency is accompanied by negative "precipitation minus evapotranspiration" and is expected to be stronger in the far future, regardless of the season (Fig. 5; see also Fig. S7). In other words, the drying trends observed over the recent

decades may continue in the coming decades, and their impacts, with high confidence, will become more significant in magnitude at the end of the twenty-first century (Figs. 2–5). The change in the seasonal cycle further supports these results. At a larger spatial scale, the meridional dipole of precipitation change implies a northward migration of the storm track. This shift will be discussed in detail in section 3d.

c. Regional climate simulations

We perform the MRCM simulations driven by the three CMIP6 models to analyze patterns of drying over the complex topography region. Consistent with the GCM projections, the MRCM shows increased risks of drying for the near-term period relative to historical levels (Fig. 6; see also Figs. S8 and S9). Notably, rainy-season precipitation may decrease by 4%–8% in high-altitude catchments by the middle of the twenty-first century, depending on the scenario. The freshwater decline in the basin will likely be more pronounced in spring than winter at the seasonal time scale. For instance, despite a prominent multidecadal variability, a modest (not significant) decrease (1%–4%) in precipitation is expected during winter. During boreal spring, precipitation could decrease by 5% and 13% under the SSP1-2.5 and SSP5-8.5 scenarios, respectively. It is important to note that the drying trend over the region is more pronounced in the selected simulations than the average of all GCM simulations (Figs. S8 and S9).

Precipitation changes are highly heterogeneous spatially, but there is high agreement across the three MRCM simulations that the headwaters region may experience a tendency toward a drier climate (Fig. 7). Spring precipitation over the region is likely to decrease by 2.7%, 7.0%, 4.2%, and 4.5% (13.6%, 13.6%, 11.3%, and 13.0%) in the low-emission (high-emission) scenario for MPI-ESM1-2-LR, HadGEM3-GC31-LL, NorESM2-LM, and their ensemble mean, respectively. Also, precipitation declines approximately in proportion to the increase in CO_2 emissions, consistent with the GCM simulations (Fig. S8). It implies that achieving net-zero emissions would significantly reduce the higher risks of drought (Figs. 6 and 7; see also Figs. S8 and S9). Although the southeast portion of the domain, around the Zagros Mountains, is likely to experience a slight increase in precipitation, there is a lack of agreement between the models.

d. Potential physical mechanisms

To better identify the potential explanations of the decrease in precipitation, it is essential to understand changes in midlatitude storm tracks (also known as extratropical cyclone tracks), which play a fundamental role in the weather/climate systems, especially precipitation regimes across the Mediterranean and Mesopotamia. In observations, most winter storms that head for Mesopotamia generally form in the Mediterranean (Hochman et al. 2022), while only a few of them originate from the North Atlantic (Fig. S10). The spring storm tracks show a similar pattern to those for winters. However, the genesis locations during the spring are distributed closer to the continental regions (Europe and North Africa) (Fig. S10).
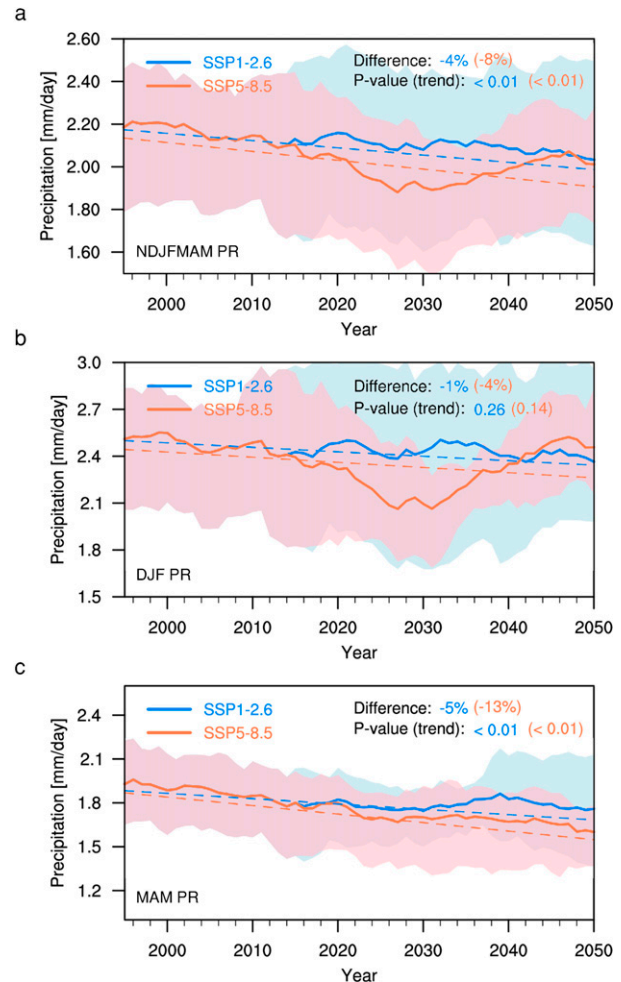

FIG. 6. Time series of seasonal-mean precipitation (PR; unit: mm day^{-1}) over the Mesopotamian headwaters for the (a) wet season [November–May (NDJFMAM)], (b) winter [December–February (DJF)], and (c) spring [March–May (MAM)] derived from an ensemble of three MRCM simulations under low (blue; SSP1-2.6) and high (red; SSP5-8.5) emission scenarios. Solid lines and shading indicate a 20-yr moving average and intermodel spread, respectively. Difference (2021–50 minus 1985–2014) in precipitation is represented in each plot. The p value for linear trend is based on a nonparametric Mann–Kendall test.

Future climate change is expected to change the nature of these storms.

A robust increase in SLP over the Mediterranean will likely weaken the storms and reduce the number of them that penetrate from the Mediterranean into Mesopotamia by the end of this century (Fig. 8). This is the main physical mechanism explaining the projected change of precipitation over Mesopotamia. In the near-term future, no robust changes in SLP are found, although models indicate a slightly higher SLP and intensified anticyclonic circulation in the Mediterranean. However, enhanced global warming in the far future would trigger robust patterns of higher SLP with an associated anticyclonic circulation centered over the Mediterranean, where most storms originate.
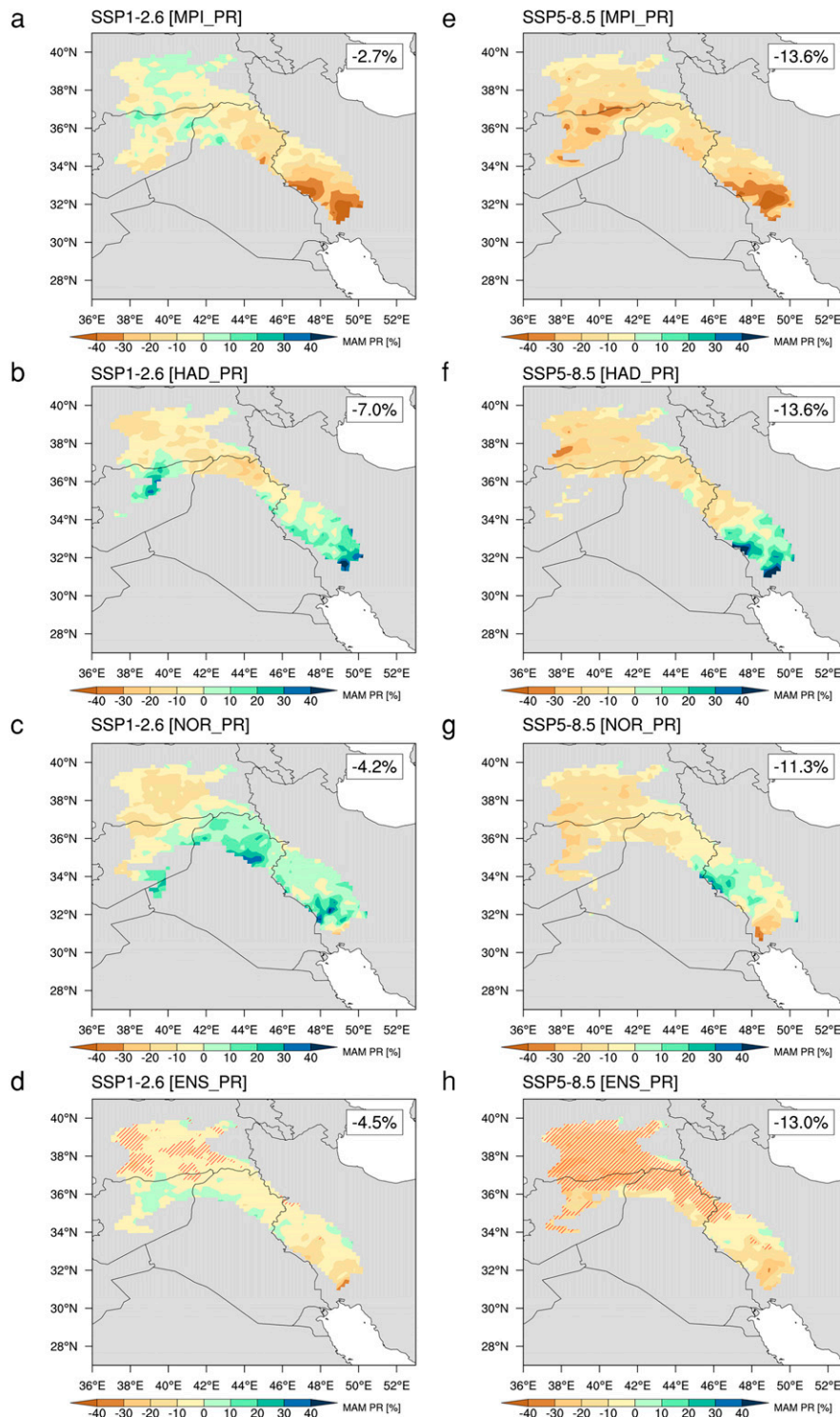
FIG. 7. Near-term changes in precipitation (PR; unit: %) during the spring (March–May; MAM) derived from three MRCM simulations (MPI, HAD, and NOR) and their ensemble mean (ENS) under (a)–(d) low (SSP1-2.6) and (e)–(h) high (SSP5-8.5) emission scenarios. Difference (2021–50 minus 1985–2014) in precipitation over the Mesopotamian headwaters (see Fig. 1c) is represented in each plot. Superimposed hatching indicates agreement (100%) by MRCM simulations on the sign of the change. Areas with annual total PR < 100 mm are masked out to avoid potential inflation due to small rainfall amounts.
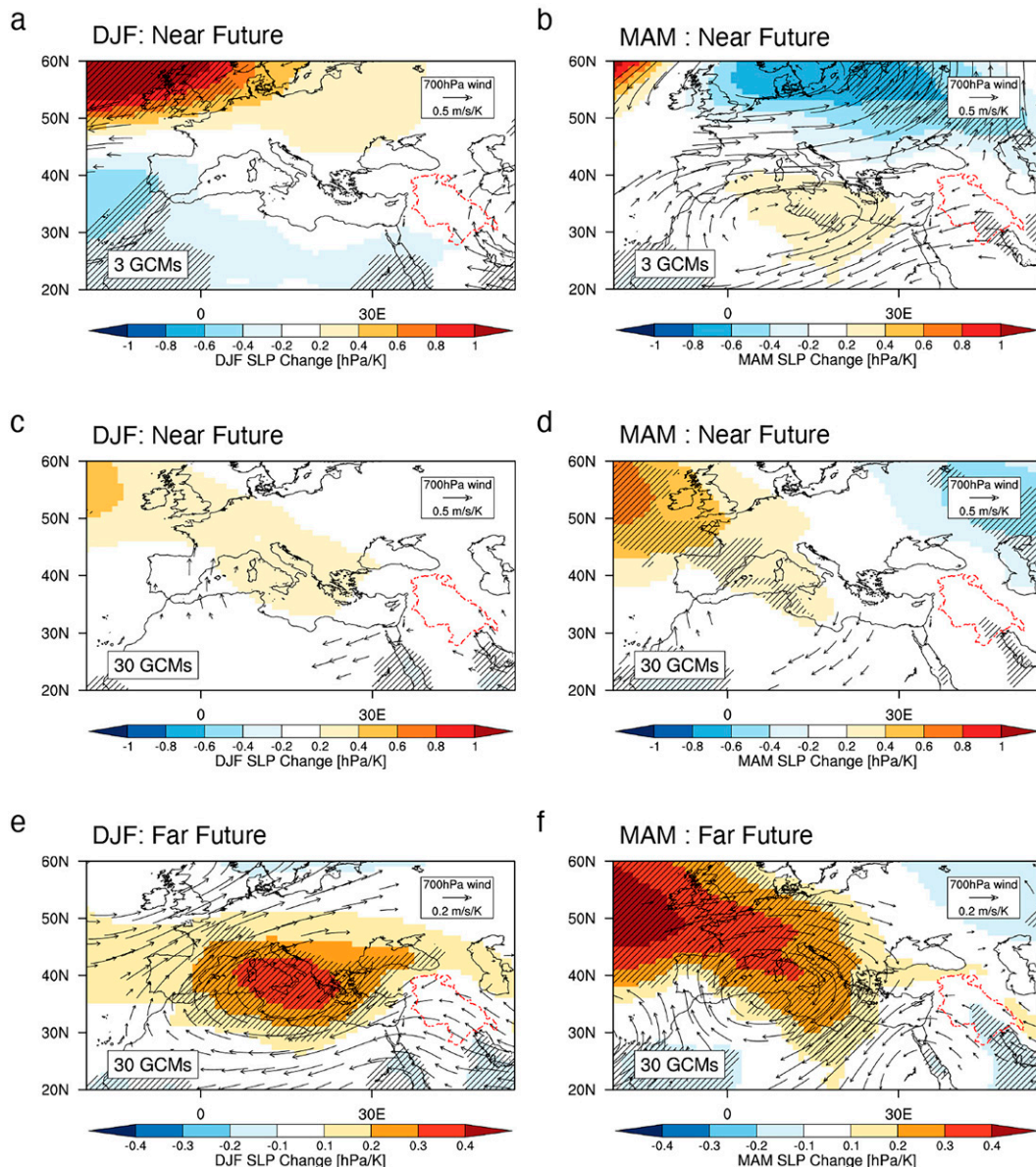
FIG. 8. Near-term changes in sea level pressure (SLP; shading; unit: hPa K^{-1}) and 700-hPa winds (vectors; unit: m s^{-1} K^{-1}) during (a),(c) DJF and (b),(d) MAM derived from ensemble of (a),(b) 3 and (c),(d) 30 CMIP6 GCMs. (e),(f) As in (c) and (d), but for the far future (2071–2100). Superimposed hatching in (a) and (b) denotes agreement (100%) by three GCMs on the sign of the change. Superimposed hatching in (c)–(f) indicates that more than 80% of models agree on the sign of the change. Wind vectors with a lack of agreement on the sign of the change by at least 100% (80%) of models are not shown in (a) and (b) [(c)–(f)]. Projections are normalized by each model's global-mean temperature change.

The higher SLP, in turn, makes storms upstream less frequent and weaker, hence causing a drying downstream.

In addition to the SLP changes, northward migration of the fewer Mediterranean storm tracks could possibly lead to precipitation decline over the Mesopotamian headwaters (Fig. 9). The three selected GCMs, unlike all GCMs, show a decrease in spring storm activity across North Africa by the midcentury

(Fig. 9b). That is, the number of storms that propagate from North Africa to Mesopotamia may possibly decrease. At the same time, the selected models also indicate an enhanced storm activity in the European continent, exhibiting a meridional dipole pattern (Fig. 9b). Such a dipole pattern is suggestive of a slight northward shift of the Mediterranean storm tracks, which implies fewer storms passing across Mesopotamia. In
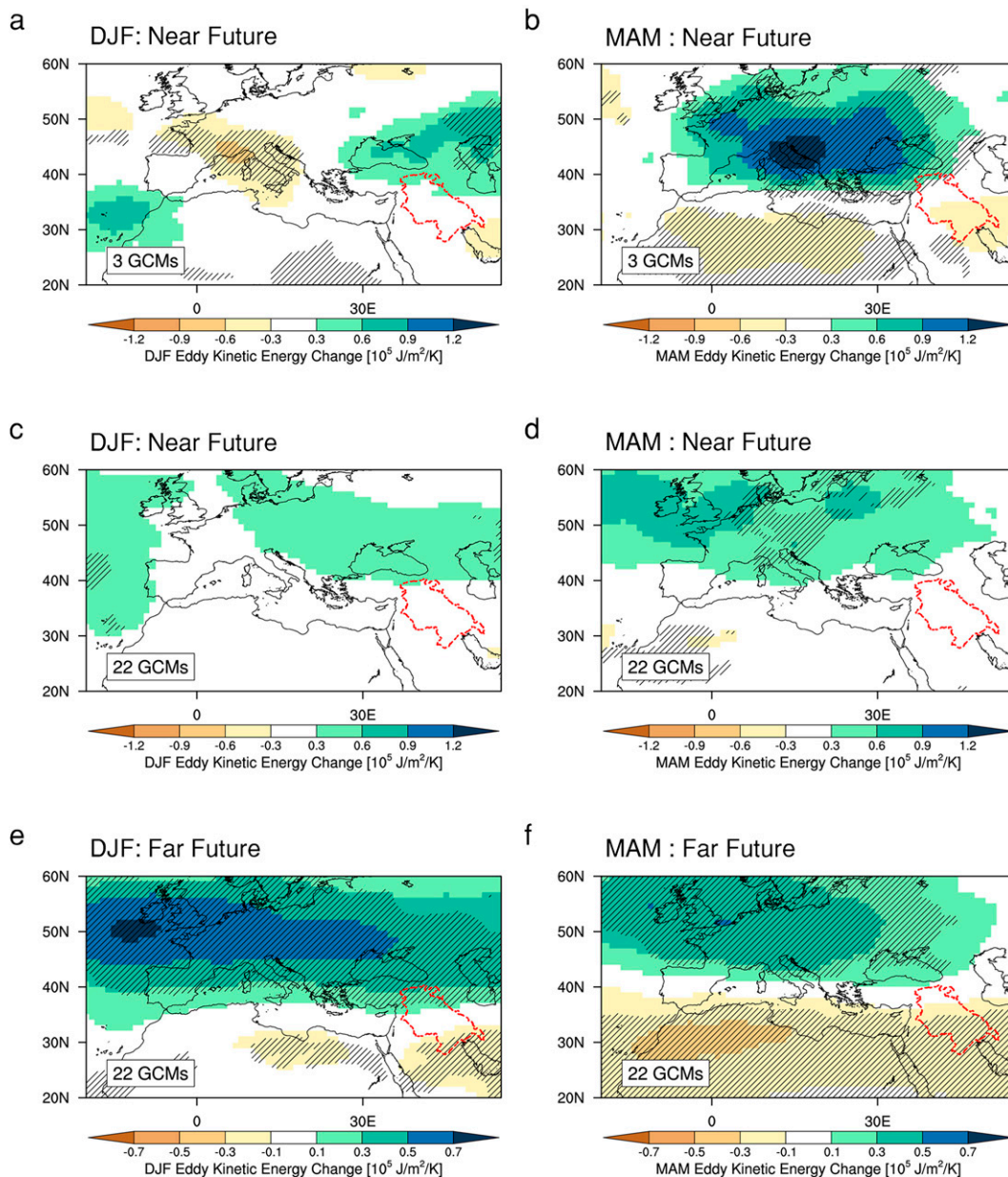
FIG. 9. Near-term changes in eddy kinetic energy (unit: 10^5 J m^{-2} K^{-1}; vertically integrated and 2–8-day bandpass filtered) during (a),(c) DJF and (b),(d) MAM derived from ensemble of (a),(b) 3 and (c),(d) 22 CMIP6 GCMs. (e),(f) As in (c) and (d), but for the far future (2071–2100). Superimposed hatching in (a),(b) denotes agreement (100%) by three GCMs on the sign of the change. Superimposed hatching in (c)–(f) indicates that more than 80% of models agree on the sign of the change. Projections are normalized by each model's global-mean temperature change.

the far future, the dipole signal will be more robust in the wet season (particularly in the spring with more drying). The pronounced intermodel spread in the near-term projections is a reason for caution, as discussed previously. However, the uncertainty in the projections by the end of the twenty-first century is significantly decreased compared to what is seen in the near-term projections.

Given that the jet stream location guides a storm path (Hoskins and Ambrizzi 1993), we suggest that a larger separation

of the polar and subtropical jets is an important contributor to the meridional shift of the storm track (Fig. 10). Projected changes in zonal flow are shown in Fig. 10. Unsurprisingly, there is a lack of consensus on the shift in the jet stream (particularly in the lower troposphere over the subtropics and extratropics) across models for the near-term future, consistent with the change in precipitation (Fig. 4). However, the jet shift is detectable during the spring in the three selected GCMs. The eddy-driven jet (i.e., polar jet) is well separated from the thermally
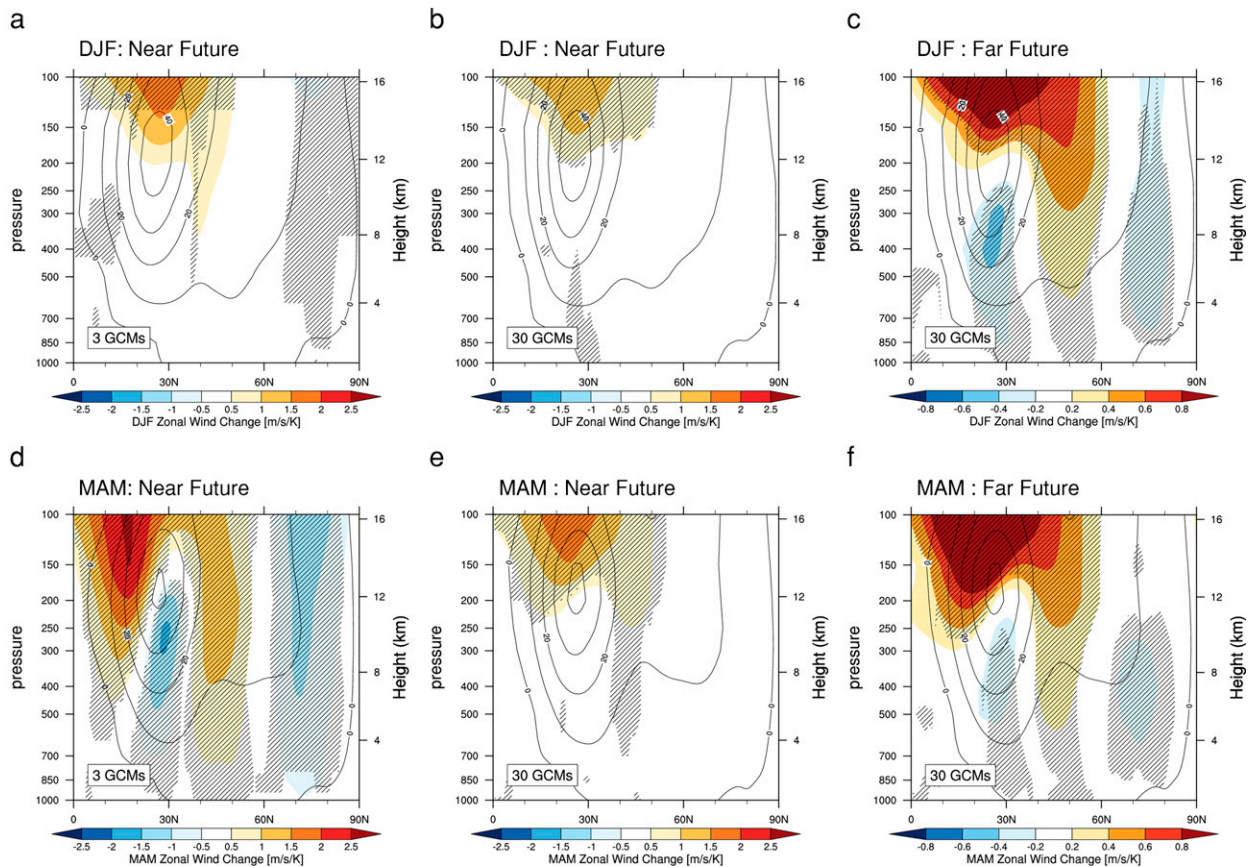
FIG. 10. Near-term changes in the zonal wind (unit: m s^{-1} K^{-1}) averaged between 0° and 50°E during (a),(b) DJF and (d),(e) MAM derived from ensemble of (a),(d) 3 and (b),(e) 30 CMIP6 GCMs. (c),(f) As in (b) and (e), but for the far future (2071–2100). Contour lines in each plot indicate climatology of zonal wind during the reference period (1985–2014). Superimposed hatching in (a) and (d) denotes agreement (100%) by three GCMs on the sign of the change. Superimposed hatching in (b), (c), (e), and (f) indicates that more than 80% of models agree on the sign of the change. Projections are normalized by each model's global-mean temperature change.

driven jet (i.e., subtropical jet over North Africa with its core at 30°N), associated with the lower-tropospheric anomalous anticyclonic circulation over the Mediterranean: the southern Mediterranean and North Africa could see decreased zonal wind speed [consistent with Zappa et al. (2015b)], but Europe is likely to experience enhanced zonal wind speed. A similar robust pattern is also found across most ensemble members of the three selected GCMs, suggesting that the jet shift is mainly driven by near-term climate change rather than internal variability (Fig. S11). As the atmospheric CO_2 concentration is increased by the end of this century, jet separation is expected in both summer and winter. At the event scale, the largest (smallest) separation of the two jets in the three selected GCMs indeed causes a poleward (equatorward) shift of the storm tracks, implying that the number of passing rainstorms from the Mediterranean/North Africa to Mesopotamia is notably reduced (increased) (Fig. 11). This mechanism is further supported by observations (Figs. S12 and S13).

4. Discussion

Consistent with our findings, most previous studies using GCMs expect a decrease in precipitation over the eastern

Mediterranean by the end of this century under high emission scenarios (Giorgi 2006; Kitoh et al. 2008; Diffenbaugh and Giorgi 2012; Wu et al. 2020). However, GCMs show poor performance in simulating climate over complex topography regions (Seneviratne et al. 2012; Flato et al. 2013; Im et al. 2017b; Fig. S4), like Mesopotamia, including multiple mountain ranges (the Zagros and Taurus Mountains) and surrounding seas (the Mediterranean Sea, the Black Sea, the Kasper Sea, the Red Sea, and the Persian Gulf). Thus, these GCM projections should be interpreted with caution. To address the issue, regional climate projections are used in this study (especially for the near-term future).

Considering the Euro-Mediterranean area, some aspects of the precipitation projections presented in this paper are similar to previous regional climate studies, expecting a dipole-like pattern characterized by wetting trends in Europe and drying trends in the Mediterranean (Zittis et al. 2019; Cherif et al. 2020; Zittis et al. 2021). However, little or no attention was paid to the Mesopotamian basin in these studies. In addition, their analysis was primarily centered on changes in mean and extreme precipitation rather than changes in atmospheric circulation.
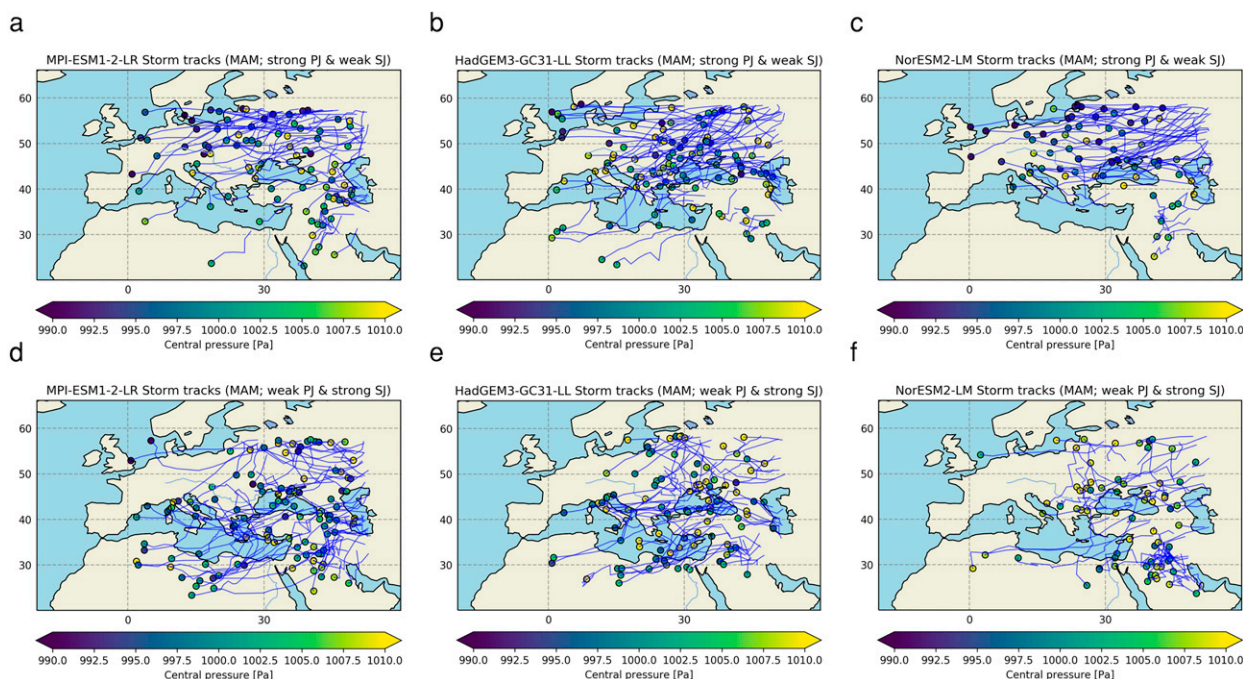
FIG. 11. (a)–(c) Storm tracks during boreal spring for near-term future (2021–50) in the case of a large separation between polar (PJ) and subtropical (SJ) jets (with the circulation index above the 90th percentile, i.e., strong PJ in the extratropics and weak SJ in the subtropics) for three models (MPI-ESM1-2-LR, HadGEM3-GC31-LL, and NorESM2-LM). (d)–(f) As in (a)–(c), but for the case of a small separation between the two jets (with the circulation index below the 10th percentile, i.e., weak PJ in the extratropics and strong SJ in the subtropics). Storm tracks are indicated by blue lines. Genesis locations with central pressure are represented by colored dots.

The comprehensive GCM projections from the two CMIP generations offer insights into the broader range of possible climate change impacts, although some caution should be exercised in interpreting the coarse-resolution GCM projections. Based on the CMIP5 and CMIP6 GCM projections, we found no consensus regarding the effect of near-future global warming on rainstorms or snowstorms in the eastern Mediterranean. Uncertainty in the near-term climate projections is notably higher in winter than spring. The discrepancy between the near-term projections can be partly explained by insufficient greenhouse gas emissions that may not overwhelm natural variability (Kelley et al. 2012; Choi et al. 2016). In particular, the high uncertainty in winter may be attributable to NAO (i.e., the dominant mode of wintertime climate variability), which might, to some extent, mask the impacts of anthropogenic climate change (Cullen and deMenocal 2000; Kelley et al. 2015).

Moreover, we propose that circulation changes in the lower troposphere play a critical role in shaping the Mediterranean precipitation changes in observations (Fig. S14) and projections (Figs. 8–11; Zappa et al. 2015b; Seager et al. 2014; Tuel and Eltahir 2020). The circulation changes are also found to be associated with the uncertainty in near-term future projections of precipitation over Mesopotamia (Fig. 12), in line with the previous findings in the literature (Zappa et al. 2015b). Correlation analysis reveals that the differences between the low-level zonal wind responses of different models are associated with the uncertainties in the near-term precipitation

projection (Fig. 12a). For example, the models, featuring a strengthened polar jet in the extratropics and a weakened subtropical jet in the subtropics, exhibit a pronounced drying trend. About 50% (p value < 0.01) of intermodel spread in the near-term projection of spring precipitation can be explained by the circulation index (see section 2b) (Fig. 12b). For the late decades of this century, the circulation index shows a tendency toward higher values than the near future, leading to the robust model consensus on the changes in the precipitation in the headwaters of the Tigris and Euphrates Rivers (Fig. 12b). Although this study mainly focuses on the dynamical response to external forcing, thermodynamic processes are also important in shaping precipitation trends over Mesopotamia (Tuel et al. 2022).

Reducing uncertainties requires more refined observations and better models (Trigo et al. 2010; Kelley et al. 2015; Pal and Eltahir 2016; Im et al. 2017a; Kang and Eltahir 2018). To alleviate this concern, this study used various observations derived from in situ data and satellite remote sensing retrievals. Based on these data, we carefully selected the best performing models in simulating the present climate conditions (mean climate and climate trends) and dynamically downscaled them using the MRCM. Note that the MRCM shows comparable or better performance in reproducing the present climate conditions, in terms of the spatial distributions of temperature and precipitation over Mesopotamia, than the forcing boundary conditions (Fig. S4). Thus, we believe that the MRCM simulations driven by the three different GCMs provide more
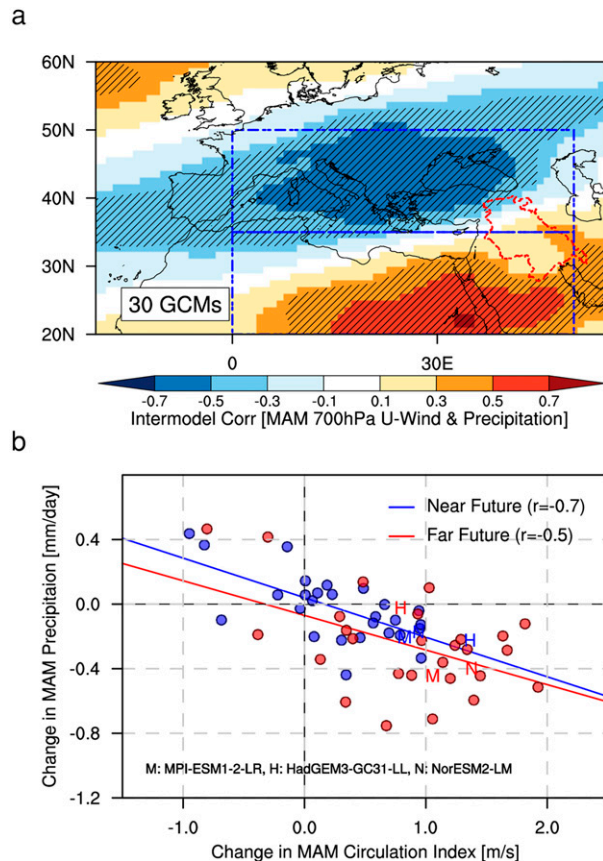
a

b

FIG. 12. (a) Correlation map between 700-hPa zonal wind responses of 30 different models to anthropogenic forcing and uncertainties (intermodel spread) in the near-term precipitation projections. Blue rectangles in (a) denote the region used to define the circulation index (see section 2b). (b) Projected changes in MAM circulation index and precipitation across CMIP6 models. The least squares regression lines are shown for the near future (2021–50; blue) and far future (2071–2100; red). Correlation coefficients (*r*) are represented in (b).

reliable future climate projections. However, we acknowledge that a lack of ground observations can pose a problem in assessing model performance adequately, and different conclusions could be reached depending on selected models.

Several lines of evidence indicate that midlatitude SST warming and high-latitude SST cooling (associated with weakened Atlantic meridional overturning circulation) are the primary drivers of an extension of the North Atlantic jet stream toward western Europe (Woollings et al. 2012; Matsumura et al. 2019; Gervais et al. 2019). Although storm activity increases from the North Atlantic to western Europe, it is unlikely to reach as far as Mesopotamia. For example, in the vicinity of the Mediterranean Sea, a northward shift of storm tracks may reduce storms penetrating from the North Atlantic to Mesopotamia through the European continent.

5. Conclusions

In recent decades, human-induced climate change may have significantly reduced precipitation over the Mesopotamian head-

waters, exacerbating the existing water deficit in the Fertile Crescent. The dwindling freshwater resource (including those caused by the impacts of wars, population growth, and upstream water diversion projects) forced many people to leave their hometowns to seek economic opportunities. Without an urgent and significant cut to greenhouse gas emissions, this region could face additional socioeconomic hardship in the future due to climate change. However, attempts at international cooperation to reach net-zero emissions by the midcentury remain elusive.

Accurately projecting the short-term impacts of climate change is critical for developing sound adaptation policies. We first considered all available CMIP5 and CMIP6 GCMs to provide insights into the broader range of possible climate change impacts and found that the near-term projection of precipitation is highly uncertain (low confidence) over Mesopotamia. To increase the reliability of near-term future predictions, we then carefully selected global and regional climate simulations. The MRCM simulations driven by the selected GCMs show that spring-season precipitation may decrease by 5%–13% in the headwaters by the midcentury, depending on the scenario (SSP1-2.6 and SSP5-8.5). Toward the end of the century, we project with high confidence a significant decrease in wet-season precipitation under the high emission scenario, implying a century-long drying trend. Note that the robustness of the drying signal across all far-future simulations is striking regardless of the CMIP phase. This study suggests that higher SLP centered on the Mediterranean Sea and the poleward migration of the fewer Mediterranean storm tracks are the likely physical mechanisms of these drying trends. Higher SLP in the central Mediterranean will likely lead to a less frequent and weaker storm over the region where most storms originate. The poleward migration of the fewer Mediterranean storm tracks could also decrease the frequency of storms that penetrates into Mesopotamia, possibly causing severe drought in Mesopotamia.

We argue that if net-zero greenhouse gas emissions are not achieved by the midcentury, the continuous decrease in precipitation over this century will exert intense pressure on the water–food–energy nexus over this region.

data are available at https://github.com/ecjoliver/stormTracking. CMIP5 (CMIP6) model output were downloaded from https://esgf-node.llnl.gov/search/cmip5/ (https://esgf-node.llnl.gov/projects/cmip6/). Regional simulations are available on request from the corresponding author.

REFERENCES

Adler, R. F., and Coauthors, 2003: The version-2 Global Precipitation Climatology Project (GPCP) monthly precipitation analysis (1979–present). *J. Hydrometeor.*, **4**, 1147–1167, https://doi.org/10.1175/1525-7541(2003)004<1147:TVGPCP>2.0.CO;2.

Bozkurt, D., and O. L. Sen, 2013: Climate change impacts in the Euphrates–Tigris Basin based on different model and scenario simulations. *J. Hydrol.*, **480**, 149–161, https://doi.org/10.1016/j.jhydrol.2012.12.021.

Chelton, D. B., M. G. Schlax, and R. M. Samelson, 2011: Global observations of nonlinear mesoscale eddies. *Prog. Oceanogr.*, **91**, 167–216, https://doi.org/10.1016/j.pocean.2011.01.002.

Cherif, S., and Coauthors, 2020: Drivers of change. *Climate and Environmental Change in the Mediterranean Basin—Current Situation and Risks for the Future: First Mediterranean Assessment Report*, W. Cramer, J. Guiot, and K. Marini, Eds., Plan Bleu, UNEP/MAP, 54–180.

Choi, Y.-W., and E. A. B. Eltahir, 2022: Heat stress during Arba'een foot-pilgrimage (World's largest gathering) projected to reach "dangerous" levels due to climate change. *Geophys. Res. Lett.*, **49**, e2022GL099755, https://doi.org/10.1029/2022GL099755.

——, and Coauthors, 2016: Future changes in drought characteristics over South Korea using multi regional climate models with the standardized precipitation index. *Asia-Pac. J. Atmos. Sci.*, **52**, 209–222, https://doi.org/10.1007/s13143-016-0020-1.

——, D. J. Campbell, J. C. Aldridge, and E. A. B. Eltahir, 2021: Near-term regional climate change over Bangladesh. *Climate Dyn.*, **57**, 3055–3073, https://doi.org/10.1007/s00382-021-05856-z.

Cullen, H. M., and P. B. deMenocal, 2000: North Atlantic influence on Tigris–Euphrates streamflow. *Int. J. Climatol.*, **20**, 853–863, https://doi.org/10.1002/1097-0088(20000630)20:8<853::AID-JOC497>3.0.CO;2-M.

Diffenbaugh, N. S., and F. Giorgi, 2012: Climate change hotspots in the CMIP5 global climate model ensemble. *Climatic Change*, **114**, 813–822, https://doi.org/10.1007/s10584-012-0570-x.

Evans, J. P., 2009: 21st century climate change in the Middle East. *Climatic Change*, **92**, 417–432, https://doi.org/10.1007/s10584-008-9438-5.

Flato, G., and Coauthors, 2013: Evaluation of climate models. *Climate Change 2013: The Physical Science Basis*, T. F. Stocker et al., Eds., Cambridge University Press, 741–866, https://doi.org/10.1017/CBO9781107415324.020.

Foley, J. A., I. C. Prentice, N. Ramankutty, S. Levis, D. Pollard, S. Sitch, and A. Haxeltine, 1996: An integrated biosphere model of land surface processes, terrestrial carbon balance, and vegetation dynamics. *Global Biogeochem. Cycles*, **10**, 603–628, https://doi.org/10.1029/96GB02692.

Gervais, M., J. Shaman, and Y. Kushnir, 2019: Impacts of the North Atlantic warming hole in future climate projections: Mean atmospheric circulation and the North Atlantic jet. *J. Climate*, **32**, 2673–2689, https://doi.org/10.1175/JCLI-D-18-0647.1.

Gianotti, R. L., 2012: Regional climate modeling over the Maritime Continent: Convective cloud and rainfall processes. Ph.D. dissertation, Massachusetts Institute of Technology, 306 pp.

——, and E. A. B. Eltahir, 2014a: Regional climate modeling over the Maritime Continent. Part I: New parameterization for convective cloud fraction. *J. Climate*, **27**, 1488–1503, https://doi.org/10.1175/JCLI-D-13-00127.1.

——, and ——, 2014b: Regional climate modeling over the Maritime Continent. Part II: New parameterization for autoconversion of convective rainfall. *J. Climate*, **27**, 1504–1523, https://doi.org/10.1175/JCLI-D-13-00171.1.

Giorgi, F., 2006: Climate change hot-spots. *Geophys. Res. Lett.*, **33**, L08707, https://doi.org/10.1029/2006GL025734.

Harris, I., T. J. Osborn, P. Jones, and D. Lister, 2020: Version 4 of the CRU TS monthly high-resolution gridded multivariate climate dataset. *Sci. Data*, **7**, 109, https://doi.org/10.1038/s41597-020-0453-3.

Hochman, A., F. Marra, G. Messori, J. G. Pinto, S. Raveh-Rubin, Y. Yosef, and G. Zittis, 2022: Extreme weather and societal impacts in the eastern Mediterranean. *Earth Syst. Dyn.*, **13**, 749–777, https://doi.org/10.5194/esd-13-749-2022.

Hoskins, B. J., and T. Ambrizzi, 1993: Rossby wave propagation on a realistic longitudinally varying flow. *J. Atmos. Sci.*, **50**, 1661–1671, https://doi.org/10.1175/1520-0469(1993)050<1661:RWPOAR>2.0.CO;2.

Huffman, G. J., and Coauthors, 2007: The TRMM Multisatellite Precipitation Analysis (TMPA): Quasi-global, multiyear, combined-sensor precipitation estimates at fine scales. *J. Hydrometeor.*, **8**, 38–55, https://doi.org/10.1175/JHM560.1.

Im, E.-S., and E. A. B. Eltahir, 2014: Enhancement of rainfall and runoff upstream from irrigation location in a climate model of West Africa. *Water Resour. Res.*, **50**, 8651–8674, https://doi.org/10.1002/2014WR015592.

——, and ——, 2018: Simulation of the diurnal variation of rainfall over the western Maritime Continent using a regional climate model. *Climate Dyn.*, **51**, 73–88, https://doi.org/10.1007/s00382-017-3907-3.

——, R. L. Gianotti, and E. A. B. Eltahir, 2014a: Improving the simulation of the West African monsoon using the MIT regional climate model. *J. Climate*, **27**, 2209–2229, https://doi.org/10.1175/JCLI-D-13-00188.1.

——, M. P. Marcella, and E. A. B. Eltahir, 2014b: Impact of potential large-scale irrigation on the West African monsoon and its dependence on location of irrigated area. *J. Climate*, **27**, 994–1009, https://doi.org/10.1175/JCLI-D-13-00290.1.

——, J. S. Pal, and E. A. B. Eltahir, 2017a: Deadly heat waves projected in the densely populated agricultural regions of South Asia. *Sci. Adv.*, **3**, e1603322, https://doi.org/10.1126/sciadv.1603322.

——, Y.-W. Choi, and J.-B. Ahn, 2017b: Worsening of heat stress due to global warming in South Korea based on multi-RCM ensemble projections. *J. Geophys. Res. Atmos.*, **122**, 11 444–11 461, https://doi.org/10.1002/2017JD026731.

Kang, S. C., and E. A. B. Eltahir, 2018: North China Plain threatened by deadly heatwaves due to climate change and irrigation. *Nat. Commun.*, **9**, 2894, https://doi.org/10.1038/s41467-018-05252-y.

Kelley, C., M. Ting, R. Seager, and Y. Kushnir, 2012: Mediterranean precipitation climatology, seasonal cycle, and trend as simulated by CMIP5. *Geophys. Res. Lett.*, **39**, L21703, https://doi.org/10.1029/2012GL053416.

Kelley, C. P., S. Mohtadi, M. A. Cane, R. Seager, and Y. Kushnir, 2015: Climate change in the Fertile Crescent and implications

of the recent Syrian drought. *Proc. Natl. Acad. Sci. USA*, **112**, 3241–3246, https://doi.org/10.1073/pnas.1421533112.

Kitoh, A., A. Yatagai, and P. Alpert, 2008: First super-high-resolution model projection that the ancient "Fertile Crescent" will disappear in this century. *Hydrol. Res. Lett.*, **2**, 1–4, https://doi.org/10.3178/hrl.2.1.

Lee, S. H., P. D. Williams, and T. H. A. Frame, 2019: Increased shear in the North Atlantic upper-level jet stream over the past four decades. *Nature*, **572**, 639–642, https://doi.org/10.1038/s41586-019-1465-z.

Marcella, M. P., 2012: Biosphere–atmosphere interactions over semi-arid regions: Modeling the role of mineral aerosols and irrigation in the regional climate system. Ph.D. dissertation, Massachusetts Institute of Technology, 282 pp.

——, and E. A. B. Eltahir, 2008: The hydroclimatology of Kuwait: Explaining the variability of rainfall at seasonal and interannual time scales. *J. Hydrometeor.*, **9**, 1095–1105, https://doi.org/10.1175/2008JHM952.1.

——, and ——, 2012: Modeling the summertime climate of southwest Asia: The role of land surface processes in shaping the climate of semiarid regions. *J. Climate*, **25**, 704–719, https://doi.org/10.1175/2011JCLI4080.1.

Matsumura, S., S. Ueki, and T. Horinouchi, 2019: Contrasting responses of midlatitude jets to the North Pacific and North Atlantic warming. *Geophys. Res. Lett.*, **46**, 3973–3981, https://doi.org/10.1029/2019GL082550.

McSweeney, C. F., R. G. Jones, R. W. Lee, and D. P. Rowell, 2015: Selecting CMIP5 GCMs for downscaling over multiple regions. *Climate Dyn.*, **44**, 3237–3260, https://doi.org/10.1007/s00382-014-2418-8.

Önol, B., D. Bozkurt, U. U. Turuncoglu, O. L. Sen, and H. N. Dalfes, 2014: Evaluation of the twenty-first century RCM simulations driven by multiple GCMs over the eastern Mediterranean–Black Sea region. *Climate Dyn.*, **42**, 1949–1965, https://doi.org/10.1007/s00382-013-1966-7.

Pal, J. S., and E. A. B. Eltahir, 2016: Future temperature in southwest Asia projected to exceed a threshold for human adaptability. *Nat. Climate Change*, **6**, 197–200, https://doi.org/10.1038/nclimate2833.

——, and Coauthors, 2007: Regional climate modeling for the developing world: The ICTP RegCM3 and RegCNET. *Bull. Amer. Meteor. Soc.*, **88**, 1395–1410, https://doi.org/10.1175/BAMS-88-9-1395.

Peleg, N., M. Bartov, and E. Morin, 2015: CMIP5-predicted climate shifts over the east Mediterranean: Implications for the transition region between Mediterranean and semiarid climates. *Int. J. Climatol.*, **35**, 2144–2153, https://doi.org/10.1002/joc.4114.

Peterson, T. C., and R. S. Vose, 1997: An overview of the Global Historical Climatology Network temperature database. *Bull. Amer. Meteor. Soc.*, **78**, 2837–2850, https://doi.org/10.1175/1520-0477(1997)078<2837:AOOTGH>2.0.CO;2.

Reale, M., and Coauthors, 2021: Future projections of Mediterranean cyclone characteristics using the Med-CORDEX ensemble of coupled regional climate system models. *Climate Dyn.*, **58**, 2501–2524, https://doi.org/10.1007/s00382-021-06018-x.

Robinson, D. A., and Coauthors, 2012: NOAA Climate Data Record (CDR) of Northern Hemisphere (NH) snow cover extent (SCE), version 1.0. NOAA National Climatic Data Center, accessed 9 April 2022, https://doi.org/10.7289/V5N014G9.

Seager, R., H. Liu, N. Henderson, I. Simpson, C. Kelley, T. Shaw, Y. Kushnir, and M. Ting, 2014: Causes of increasing aridification of the Mediterranean region in response to rising greenhouse gases. *J. Climate*, **27**, 4655–4676, https://doi.org/10.1175/JCLI-D-13-00446.1.

Seidel, D. J., Q. Fu, W. J. Randel, and T. J. Reichler, 2008: Widening of the tropical belt in a changing climate. *Nat. Geosci.*, **1**, 21–24, https://doi.org/10.1038/ngeo.2007.38.

Seneviratne, S. I., and Coauthors, 2012: Changes in climate extremes and their impacts on the natural physical environment. *Managing the Risks of Extreme Events and Disasters to Advance Climate Change Adaptation*, C. B. Field et al., Eds., Cambridge University Press, 109–230.

Trigo, R. M., C. M. Gouveia, and D. Barriopedro, 2010: The intense 2007–2009 drought in the Fertile Crescent: Impacts and associated atmospheric circulation. *Agric. For. Meteor.*, **150**, 1245–1257, https://doi.org/10.1016/j.agrformet.2010.05.006.

Tuel, A., and E. A. B. Eltahir, 2020: Why is the Mediterranean a climate change hot spot? *J. Climate*, **33**, 5829–5843, https://doi.org/10.1175/JCLI-D-19-0910.1.

——, and ——, 2021: Mechanisms of European summer drying under climate change. *J. Climate*, **34**, 8913–8931, https://doi.org/10.1175/JCLI-D-20-0968.1.

——, Y.-W. Choi, D. AlRukaibi, and E. A. B. Eltahir, 2022: Extreme storms in Southwest Asia (northern Arabian Peninsula) under current and future climates. *Climate Dyn.*, **58**, 1509–1524, https://doi.org/10.1007/s00382-021-05975-7.

United Nations, 2019: World population prospects 2019. UN Department of Economic and Social Affairs Population Division, accessed 4 April 2022, https://population.un.org/wpp/.

Voss, K. A., J. S. Famiglietti, M. Lo, C. de Linage, M. Rodell, and S. C. Swenson, 2013: Groundwater depletion in the Middle East from GRACE with implications for transboundary water management in the Tigris–Euphrates–western Iran region. *Water Resour. Res.*, **49**, 904–914, https://doi.org/10.1002/wrcr.20078.

Winter, J. M., J. S. Pal, and E. A. B. Eltahir, 2009: Coupling of Integrated Biosphere Simulator to Regional Climate Model version 3. *J. Climate*, **22**, 2743–2757, https://doi.org/10.1175/2008JCLI2541.1.

Woollings, T., J. M. Gregory, J. G. Pinto, M. Reyers, and D. J. Brayshaw, 2012: Response of the North Atlantic storm track to climate change shaped by ocean–atmosphere coupling. *Nat. Geosci.*, **5**, 313–317, https://doi.org/10.1038/ngeo1438.

Wu, W.-Y., M.-H. Lo, Y. Wada, J. S. Famiglietti, J. T. Reager, P. J.-F. Yeh, A. Ducharne, and Z.-L. Yang, 2020: Divergent effects of climate change on future groundwater availability in key mid-latitude aquifers. *Nat. Commun.*, **11**, 3710, https://doi.org/10.1038/s41467-020-17581-y.

Yilmaz, Y. A., O. L. Sen, and U. U. Turuncoglu, 2019: Modeling the hydroclimatic effects of local land use and land cover changes on the water budget in the upper Euphrates–Tigris basin. *J. Hydrol.*, **576**, 596–609, https://doi.org/10.1016/j.jhydrol.2019.06.074.

Yin, J. H., 2005: A consistent poleward shift of the storm tracks in simulations of 21st century climate. *Geophys. Res. Lett.*, **32**, L18701, https://doi.org/10.1029/2005GL023684.

Zappa, G., M. K. Hawcroft, L. Shaffrey, E. Black, and D. J. Brayshaw, 2015a: Extratropical cyclones and the projected decline of winter Mediterranean precipitation in the CMIP5 models. *Climate Dyn.*, **45**, 1727–1738, https://doi.org/10.1007/s00382-014-2426-8.

——, B. J. Hoskins, and T. G. Shepherd, 2015b: The dependence of wintertime Mediterranean precipitation on the atmospheric

circulation response to climate change. *Environ. Res. Lett.*, **10**, 104012, https://doi.org/10.1088/1748-9326/10/10/104012.

Zittis, G., P. Hadjinicolaou, M. Klangidou, Y. Proestos, and J. Lelieveld, 2019: A multi-model, multi-scenario, and multi-domain analysis of regional climate projections for the Mediterranean. *Reg. Environ. Change*, **19**, 2621–2635, https://doi.org/10.1007/s10113-019-01565-w.

——, A. Bruggeman, and J. Lelieveld, 2021: Revisiting future extreme precipitation trends in the Mediterranean. *Wea. Climate Extreme*, **34**, 100380, https://doi.org/10.1016/j.wace.2021.100380.